

A Compact Direct Detection Receiver for L-band STAR Radiometry

Line van Nieuwstadt, Roger De Roo, David Boprie, Ron Rizor, Peter Hansen, Anthony W. England, Hanh Pham and Boon Lim

Space Physics Research Laboratory, The University of Michigan, 2455 Hayward Street, Ann Arbor MI 48109-2143

Abstract — An L-band total power receiver for use in a synthetic thinned array radiometer (STAR) is described. The total power architecture of a radiometer receiver requires special considerations to control gain fluctuations due to small temperature drifts. The STAR application requires consistent passband and stable phase between receivers. The design presented incorporates direct detection to eliminate distributed local oscillators for phase stability, distributed ceramic interference reject filters for passband consistency and temperature compensating attenuators for gain stability. The receiver is packaged in a unique “winged-hex” shape to enable close packaging with the STAR antennas and to facilitate thermal management. The resulting low cost, compact receiver is made from COTS components.

I. INTRODUCTION

Radiometric signals in the 1400 to 1427 MHz radio astronomy bands have special importance as a remote sensing technology with high sensitivity to soil moisture and sea surface salinity. Unfortunately, the long 21cm wavelength makes narrow beams for imaging from earth orbit a significant technical challenge. Synthetic Thinned Array Radiometry (STAR) is one possible technique for imaging which appears to be most viable for scaling into a space-based earth remote sensing mission. Indeed, this technique is the basis for the Very Long Baseline Array (VLBA) in New Mexico [1] and is the technique employed for the European Space Agency (ESA) Soil Moisture and Ocean Salinity (SMOS) mission [2].

The STAR concept employs a number of identical antennas each connected to a receiver. The power detected by each of these receivers is a linear function of the overall average brightness filling the antenna beam pattern. The cross-correlation of the pre-detected voltages of different receivers, or visibility, is proportional to a spatial Fourier component of the scene brightness. By appropriate location of the antenna phase centers, a set of spatial Fourier components can be measured which can be transformed in post-processing to produce a brightness image with much higher resolution than that of the antennas in the array.

This paper describes a design for the RF components (antenna output to ADC input) for the STAR-Light instrument, a ten element, 2D STAR to be used on a light aircraft for hydrological studies of the Arctic tundra [3]. The total power direct detection STAR approach imposes a number of unique requirements onto the receiver design.

1) Phase stability. A change of phase of S_{21} of a receiver results directly in a phase shift in all the visibilities associated with that receiver. Phase shifts as small as 1° can result in image smearing beyond acceptable limits. For heterodyne reception, the local oscillators of each receiver must be locked together, or a common LO must be distributed. In a large STAR, with several hundred receivers, this is a significant challenge. Direct detection eliminates the problems of distributed local oscillators, but it raises its own challenges [4].

2) Gain stability. Gain drifts appear at a radiometer output indistinguishable from signal level changes. The entire amplifier chain is budgeted to 0.0003dB rms gain changes between calibrations, typically every 2s. At the required system gain of 87dB, the overall temperature coefficient is -0.08dB/K . A combination of tight thermal control and a reduction of the thermal coefficient must be employed to meet the objective.

3) Passband consistency. Passband mismatches among receivers lead directly to a reduction in the visibility even if both receivers are stable in gain and phase. Bandpass characteristics also provide interference rejection, and the overall design of the frequency response of the amplification chain requires a balance between these requirements.

4) Size and shape. The receiver must be in close proximity to the antenna for stable and low noise operation. As STAR antennas are typically spaced from 0.5λ to 0.9λ , this requires tight packaging. In addition, the optimal shape of a 2D STAR array is that of a Y. A specialized shape enables tight spacing of the receivers immediately behind the antennas yet retains a low profile.

In addition, the radiometer application implies the usual receiver requirements, such as low noise figure, compact design and low return losses, and calibration signal

injection. The design and construction of two prototypes of the RF chain has been completed, and end-to-end testing of the entire RF chain is ongoing.

II. RECEIVER DESCRIPTION

The STAR-Light receiver detects radio brightness signals at L-band at power levels of -104 to -100 dBm. The ADC chosen for the STAR-Light receivers requires RF input power around -10 dBm, and the science application requires a receiver noise figure of less than 3.5 dB. Thus the gain block must produce 87 dB of gain, while keeping the gain very stable over integration periods that are typically 2 s long.

The gain block must also provide sufficient filtering to prevent RFI. Possibly the two most severe filtering requirements are for the transponder on the aircraft and for air traffic control radars. The transponder, required by the FAA for operations in the national air space, must transmit at least $+48$ dBm at 1090 MHz, and by necessity, is very close to the radiometer. Air Route Surveillance Radars transmit very high powers, up to $+97$ dBm, and at 1250 to 1350 MHz, very close to the radio astronomy window.

Finally, the RF circuit of the receiver must allow for multiple calibration inputs to characterize the gain, receiver noise temperature, and relative phase between receiver chains.

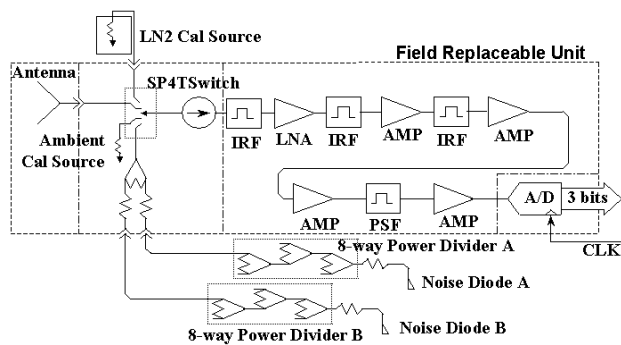


Fig. 1: RF block diagram of the direct detection STAR-Light receiver.

The design that satisfies these requirements is shown schematically in Fig. 1. At the very front end, a pair of cascaded latching electromechanical switches select one of four inputs: an antenna, an internal warm calibration load, an external cold calibration load, and a correlated noise input which can come from either of two noise diode distribution networks. An isolator and wide bandwidth ceramic filter prior to the input of a Low Noise Amplifier (LNA) protect the LNA from saturation due to RFI. Subsequent stages use alternating ceramic filters for

further RFI mitigation, attenuators for matching inputs and outputs, and a gullwing amplifier used in the wireless industry. The last filter, designated the Pre-Sample Filter (PSF), is the largest filter in the receiver with 6 stages and measuring 6.15 cm x 1.59 cm x 1.07 cm.

The primary challenge in the receiver system design is the feasibility of fabricating multiple (at least ten receivers for this STAR instrument) identical receivers. The primary design drivers for this receiver are cost, delivery time, performance, size and weight, in that priority. For each component, a matrix of available COTS parts was generated. Early in the development phase, key components such as the relays, amplifiers and filters were procured, and their performance tested over temperature. From this thermal data, the block diagram was generated using components that would meet the gain and NF requirements, as well as the temperature stability and RFI requirements.

III. GAIN STABILITY TECHNIQUES

Each amplifier has a gain temperature coefficient of -0.02 dB/K and is the component with the largest total contribution to the receiver gain temperature coefficient. The power amplifiers had a very stable gain temperature coefficient, as can be seen in the consistent slopes of the measured gain vs. temperature curves shown in Fig. 2.

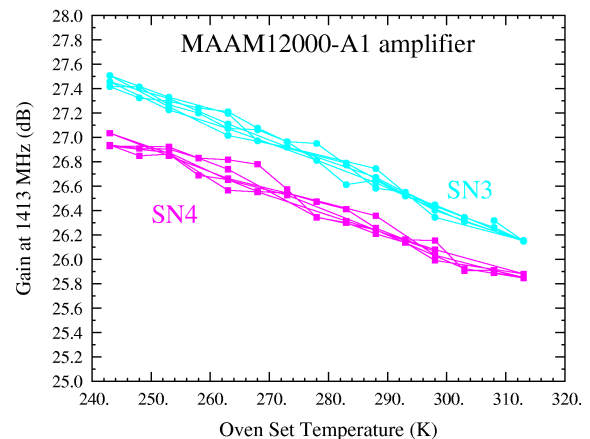


Fig. 2: Gain variations of the receiver power amplifiers as a function of temperature. Shown are measurements for two individual amplifiers over several thermal cycles.

The LNAs required a burn-in to stabilize their gain characteristics. As a result of the cascade of all the required components within the gain block, including filters, the system temperature coefficient is between -0.092 dB/K and -0.104 dB/K.

While strict thermal control is a given, it is not possible to maintain temperatures to within much better than 20mK without very extensive active control, component by component. In order to achieve the desired gain stability, the attenuators used between amplification stages to assist with matching are replaced with temperature compensating attenuators. A reduction of the entire gain chain temperature coefficient to +/- 0.015dB/K is the goal.

IV. PASSBAND CONSISTENCY

Ceramic filters manufactured by Integrated Microwave were chosen for their compact size. The size is important not only to keep the entire instrument within size and weight constraints, but to enable thermal control on a modest power budget. Large bulky cavity filters are the filters of choice for microwave radiometers, but they must be hand tuned and are highly sensitive to temperature. SAW filter technology would be desirable for this application, but development costs are very high.

Thermal tests revealed a slight insertion loss temperature coefficient of 0.0019 +/- 0.0001 dB/K per stage, of which there are 17 stages in each receiver. The filter center frequency of the PSF, which has 6 stages, did show some temperature dependence, but the -24dB skirts, which define the sampled bandwidth, did not move by more than 2MHz over a 70K range after thermal burn-in. Digital filtering will be employed downstream of the ADC to define the instrument bandwidth within the filter bandwidth.

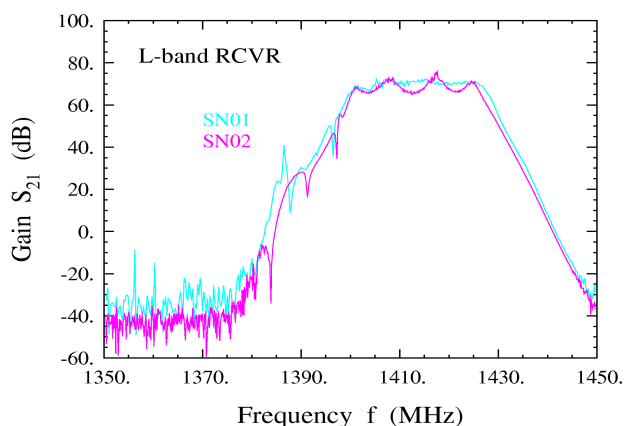


Fig. 3: Preliminary end-to-end receiver passband for two receivers. The gain has been specifically reduced to 70dB to prevent saturation of the temporary detectors. The passband ripple in SN02 is due to coupling of the high power back end with the low power front end of the receiver, and can be reduced with microwave absorber above the microstrip. The fringe wash function of these two receivers as shown is 0.830.

In addition to the stability requirements, the filters must exhibit channel-to-channel consistency. This consistency can be quantified through the fringe wash function (FWF) [5]-[6], given as

$$r(\tau) = e^{-j2\pi f_0 \tau} \int_0^\infty H_1(f) H_2^*(f) e^{j2\pi f \tau} df$$

where $r(\tau)$ is the FWF at time delay τ . $H(f)$ is the normalized frequency response for channels 1 and 2. The FWF at delay $\tau=0$ should ideally be 1, and this can occur if the two channels' frequency responses are identical, that is $H_1(f)=H_2(f)$. Measurements of the frequency responses of five the PSF prototypes yield FWF calculations for each pair of filters, for which the worst case FWF has a value of 0.996 at zero time lag. Preliminary measurements of the overall receiver passbands are shown in Fig. 3 for two receivers. The overall receiver FWF at zero lag from these measurements is 0.830.

V. SIZE AND SHAPE

The shape of a 2D STAR antenna array that appears to optimize the number of non-redundant visibilities for a given number of antennas is that of a Y [7]. The widest spacing for such a configuration for which there are no grating lobes is 0.577λ , and while the alias-free field of view shrinks to nothing at an antenna spacing of 1λ . For optimal performance of a radiometer, the antenna must be in close proximity to the receiver input, and so these antenna spacing requirements define the overall size for the receiver. The Y shape strongly suggests a hexagonally shaped receiver, however, as can be seen in Fig 4, two of

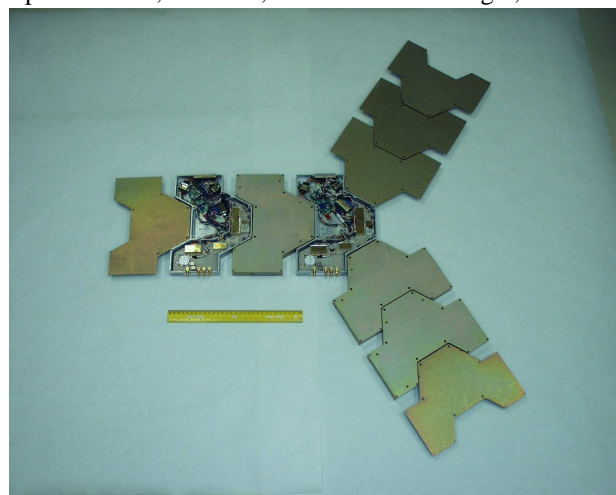


Fig 4: Arrangement of ten receivers into a 2D STAR array. Antenna housings (not shown) are hexagonally shaped and mount directly above the hexagonal portion of the receivers.

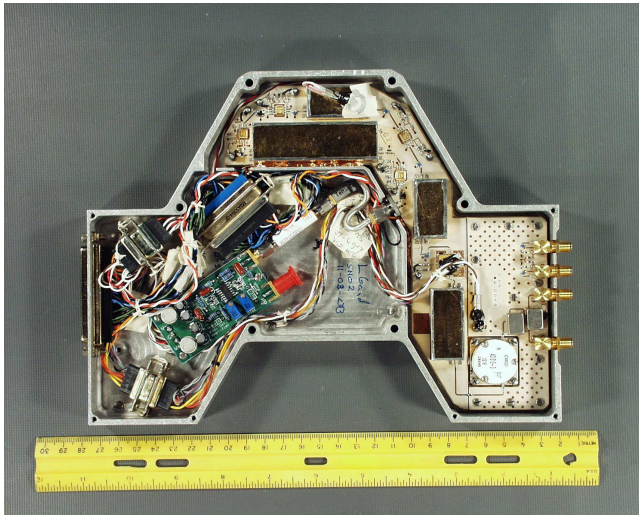


Fig. 5: Individual direct detection STAR receiver. Antenna and calibration inputs are on the right. Amplification and filtering stages occur on the right and top of the receiver. The Pre-Sampling Filter (PSF) is the largest of four ceramic filters at the top center. High speed ADC will occur in the central and left portions of the receiver although this photograph shows a detector circuit for testing and validation in that location.

the walls of the hexagon can be pushed out to make more room for the circuit. The figure shows how individual receivers interleave to form the array. The center to center spacing for this array is 14.4cm, or 0.683λ , which yields an alias-free field of view of $\pm 35^\circ$ for the STAR-Light instrument.

Within the overall shape of a “winged-hex” receiver shell, the space is subdivided roughly in half for the RF components and the ADC and supporting digital circuitry. The digital portion of the receiver is under development, but in the meantime traditional detection circuitry is used in its place so that robustness of the RF chain can be tested in a field setting. In Fig. 5, the detection circuitry is shown occupying the digital side of the receiver, while the components of the schematic in Fig. 1 fill the RF side (to the right and top in the figure).

VI. CONCLUSION

An L-band gain chain is presented which satisfies the stringent requirements for operation as a total power, direct detection STAR receiver. Special attention has been given to gain stability and passband consistency, and the design achieves 87dB of gain at 1.4GHz with an overall

gain tempo of $\pm 0.015\text{dB/K}$. The passband consistency is dominated by that of the narrowest filters in gain and filtering chain, which are 6 stage ceramic filters that exhibit a FWF at zero lag of 0.996 or better, yielding a preliminary end-to-end receiver FWF of 0.830. The gain chain is packed into a custom “winged-hex” shape that allows the receivers to be placed directly behind the antennas in a 2D STAR array.

ACKNOWLEDGEMENT

This work is supported by NSF grant OPP-0085176 from the Office of Polar Programs. The authors wish to acknowledge the assistance of the University of Michigan Space Physics Research Laboratory technical staff, and of the following students: Alina Chu, Adam Zeeb, Peter Caralis, Lisa Lau, Steven Lanzisera, James Glettler and Bill Stewart.

REFERENCES

- [1] A. R. Thompson, J. M. Moran and G. W. Swenson, *Interferometry and Synthesis in Radio Astronomy*, New York: Wiley, 1986.
- [2] Y. H. Kerr, P. Waldteufel, J.-P. Wigneron, J.-M. Martinuzzi, J. Font and M. Berger, "Soil Moisture Retrieval from Space: The Soil Moisture and Ocean Salinity {(SMOS)} Mission," *IEEE Trans. Geoscience and Remote Sensing.*, vol. 39, no. 8, pp. 1729--1735, August 2001.
- [3] A. W. England and R. De Roo, "STAR-Light: An enabling technology for modeling Arctic land surface hydrology," *2002 IEEE Geoscience and Remote Sensing Sym.*, June 2002.
- [4] M. A. Fischman and A. W. England, "Sensitivity of a 1.4 GHz Direct-Sampling Digital Radiometer," *IEEE Trans. Geoscience and Remote Sensing*, vol. 37, no. 5, pp. 2172—2180, September 1999.
- [5] F. Torres, A. Camps, J. Bara and I. Corbella. "Impact of receiver errors on the radiometric resolution of large two-dimensional aperture synthesis radiometers," *Radio Science*, vol. 32, no. 2, pp. 629—641, March-April 1997.
- [6] M. A. Fischman, A. W. England and C. S. Ruf, "How Digital Correlation Affects the Fringe Washing Function in L-band Aperture Synthesis Radiometry," *IEEE Trans. Geoscience and Remote Sensing*, vol. 40, no. 3, pp. 671—679, March 2002.
- [7] A. Camps, J. Bara, I. C. Sanahuja and F. Torres, "The Processing of Hexagonally Sampled Signals with Standard Rectangular Techniques: Application to 2-D Large Aperture Synthesis Interferometric Radiometers," *IEEE Trans. Geoscience and Remote Sensing.*, vol. 35, no. 1, pp. 183—190, January 1997.